Journal of Physics: Conference Series

Exotic cluster structures in the mean-field theory

Journal of Physics: Conference Series **445** (2013) 012036 doi:10.1088/1742-6596/445/1/012036

Exotic cluster structures in the mean-field theory

M A Klatt[1], T Ichikawa[2], K Iida[3], N Itagaki[2], J A Maruhn[4], K Matsuyanagi[2,5], K Mecke[1], S Ohkubo[6,7], P-G Reinhard[1] and B Schuetrumpf[4]

[1] Institut fuer Theoretische Physik, Universitaet Erlangen-Nuernberg, 91058 Erlangen, Germany
[2] Yukawa Institute for Theoretical Physics, Kyoto University, Kyoto 606-8502, Japan
[3] Department of Natural Science, Kochi University, 2-5-1 Akebono-cho, Kochi 780-8520, Japan
[4] Institut fuer Theoretische Physik, Universitaet Frankfurt, 60438 Frankfurt, Germany
[5] RIKEN Nishina Center, Wako 351-0198, Japan
[6] Research Center for Nuclear Physics, Osaka University, Ibaraki, Osaka 567-0047, Japan
[7] University of Kochi, Eikokuji-cho, Kochi 780-8515, Japan

Email: maruhn@th.physik.uni-frankfurt.de

Abstract. Investigations of exotic cluster-like phenomena in the framework of the Skyrme-Hartree-Fock approach are reported. The occurrence of highly excited isomeric states is discussed in connection with the question of their stability in static and time-dependent Hartree Fock (TDHF) calculations. We find rotational stabilization of a 4α chain structure in ^{16}O occurring for a limited range of angular momenta. A toroidal configuration of ^{40}Ca was also stabilized by rotation and provides a very interesting example of rotation about a symmetry axis with a strictly quantized total angular momentum. Finally we look at the formation of nuclear pasta phases in a time-dependent approach and their classification.

1. Complex isomeric states in Hartree-Fock calculations

In an early paper on cluster structure of light nuclei [1] it was already found that in Hartree-Fock calculations exotic configurations can appear that appear to be as stable as the ground state but upon closer examination are found to in reality be unstable against some type of collective deformation.

Fig. 1 illustrates how this works in practice: a chain configuration of three α-particles remains stable for several thousand static iterations in a Hartree-Fock code but then suddenly switches over to the ground state of ^{12}C via a bending deformation described by the Q_{31} multipole accompanied by a drastic change in quadrupole deformation β. It is especially interesting in this context that the typical convergence criteria like the relative change in energy per iteration ΔE and uncertainty in the single-particle energies Δh are at the same level for the chain state as for the ground state.

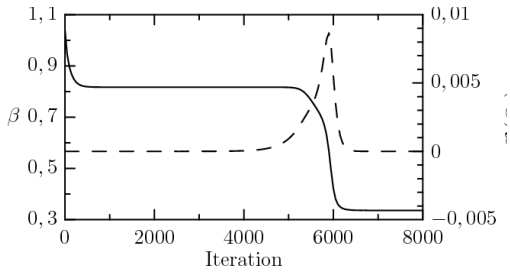

Figure 1. Quadrupole (full curve) and bending deformation (dashed) as functions of iteration number.

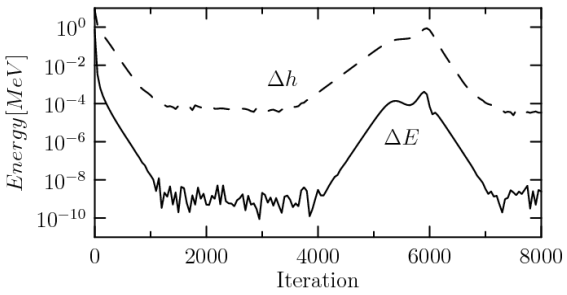

Figure 2. Convergence criteria as functions of iteration number

The reason for this behavior is not fully understood yet. It may depend on the numerical algorithm to what extent symmetries – like in this case axial symmetry – are preserved. Starting the calculation with a three α-particles not arranged on a line led to slow increase of bending and then transition into the compact shape. On the other hand, a dynamic distortion showed that instability is not instantaneous but only happens after several oscillations: it appears that just any excitation breaking axial symmetry is not enough but a more specific bending mode has to be present which comes in owing to the nonlinear coupling between these modes.

2. Stabilization of the 4α-chain state

In a recent paper [2] (discussed also in [3]) we investigated the possible stabilization of such α-chains by rotation. For that purpose static Hartree-Fock calculations with a cranking constraint were performed. The initial configuration consisted of three or four α-particles not completely collinear to avoid spurious persistence of axial symmetry and see whether the particles would be pulled onto the axis by the centrifugal force. The initial configuration is illustrated in Fig. 3(a).

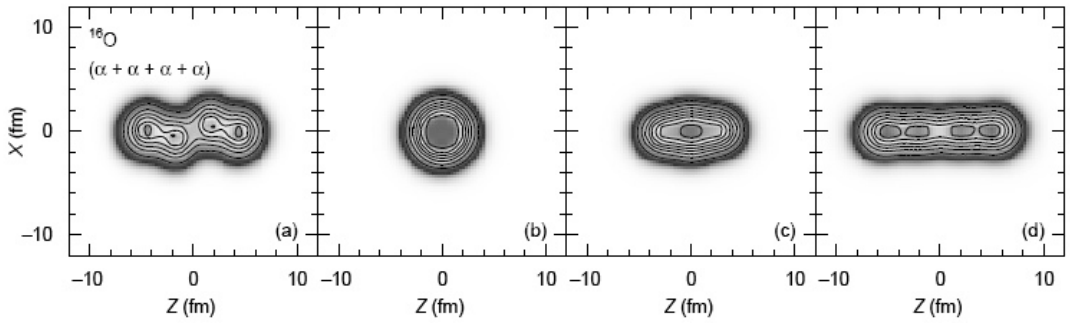

Figure 3. Initial state and different final configurations for the rotating 4α-chain.

For the ^{12}C chain state no stabilization was observed: for slow rotation the chain folded back into the compact configuration, while for fast rotation fission occurred.

Depending on the angular frequency used in the cranking constraint, for the ^{16}O case various final configurations are achieved. Fig. 4 shows which of the configurations shown in Fig. 3 is achieved at different cranking ω by plotting the rotational energy factor as a function of iteration. The most interesting of these is (d), which corresponds to the configuration being stretched into the chain by rotation. The lowest curve in the figure corresponds to fission.

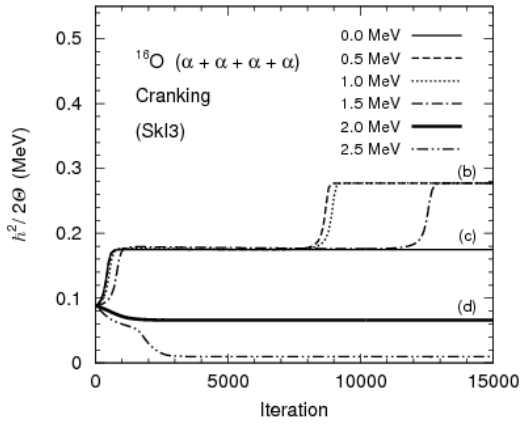

Figure 4. Convergence to different final deformations depending on ω.

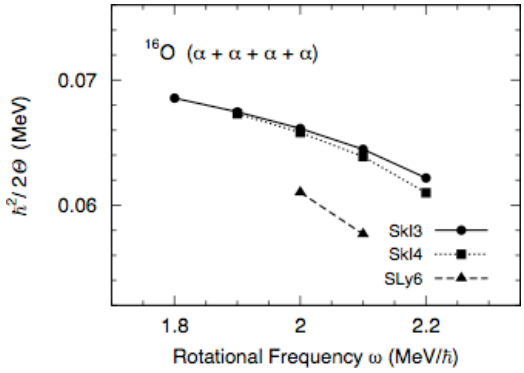

Figure 5. Rotational energy factor vs. ω for three different Skyrme forces.

The moment of inertia was calculated in two ways: from the angular momentum divided by ω and from the rigid-body expression. Both yielded essentially the same values for the chain configuration, which is not surprising considering the large deformation.

The final result for the chain configuration is shown in Fig. 5. It clearly shows that both the range of stable frequencies and the size of the deformation differ significantly between the SkI3/4 and Sly6 cases. Centrifugal stretching is also noticeable.

Time-dependent calculations were also performed for a ^{8}Be+^{8}Be collision and showed that for suitable initial orientations of the nuclei the chain state could appear as a long-lived (> 1000 fm/c) intermediate state.

3. Torus stabilization by rotation

A more exotic scenario is that of a nuclear torus as originally suggested by C. Y. Wong [4], their collective rotation and possible stabilization effects was also studied in [5,6], where, however, rigid-body rotation was assumed. For an ideally axisymmetric torus such a rotation about its symmetry axis is forbidden in quantum mechanics. There is an alternative in such cases via the alignment of the single-particle orbital and spin angular momenta producing a collective rotation as already suggested by Bohr and Mottelson [7] and realized in *K*-isomers. In contrast to rigid-body rotation this leads to a strongly quantized total angular momentum of the nucleus.

In a first investigation [8] we examined the nucleus ^{40}Ca in a rotating toroidal configuration. This was achieved by initializing a cranked static Hartree-Fock calculation with a ring of 10 α-particles. It was found that for a certain range of cranking frequencies ω a torus configuration with azimuthal symmetry was achieved. The quantal angular momentum, however, was constant over a wide range of values of ω. Fig. 6 illustrates the general behavior for different ω: for slow rotation. The values of J appearing are 20, 60, and 100, but only for J=60 the configuration remains stable for a very large number of iterations. The values occurring here can be understood quite simply from the radially displaced harmonic oscillator model [9]. In practice the wave functions can be approximated quite well as Gaussians in the distance from the central circle of the torus, and by azimuthal factors like exp(i*m*ϕ). The two spin orientations are almost degenerate. The total angular momentum is then generated by an asymmetric occupation of 10 *m*-values with four nucleons for each state. Occupying m from -4 to +5 yields a total projection of 20, for -3 to +6 we get 60, and for -2 to +7 finally a value of 100 results. This explains the large jump in projection values observed. It is made a bit smoother once spin is included, but the basic features are apparent in this way.

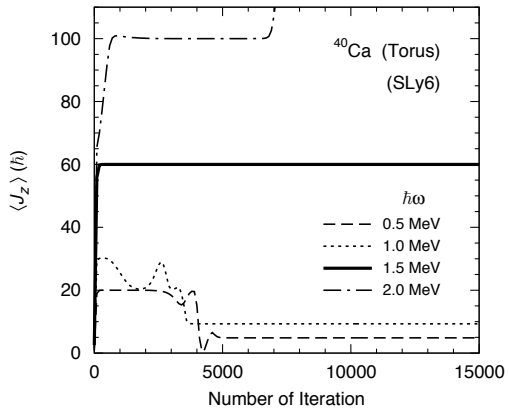

Figure 6. Convergence of angular momentum for the torus for different constraint ω.

The true stability of the configuration at J=60 is not easy to establish in static calculations, although starting with a distorted ring-like configuration showed convergence back to azimuthal symmetry for some range of distortion magnitudes. Therefore also a dynamic calculation was done to check how resilient the torus is with respect to a time-dependent sausage-like perturbation. In practice a positive time-dependent external potential was applied to act as a disrupting mechanism. It was of Gaussian shape with σ=1.8 fm and temporally also had a Gaussian profile with the duration of 20 fm/c. For a peak value of 40 MeV there was still no break-up of the torus but an initial disturbance was quickly repaired. For larger values, however, the ring broke up. The sequence of shapes shown in Fig. 7 illustrates this and also shows the collective rotation: the point of disruption clearly moves in a counter-clockwise direction.

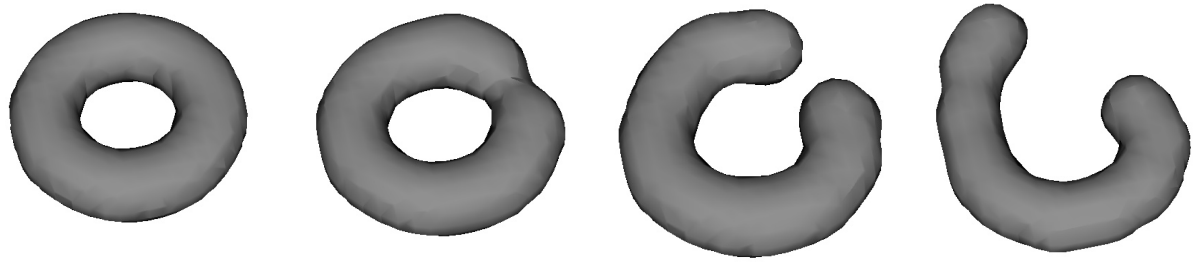

Figure 7. Sequence of shapes for the rotating torus when an external potential causes a break-up. The external potential acts at the right-hand side of the torus.

If the state with the torus configuration is formed at J = 60, the macroscopic circulating current strongly violates the time-reversal symmetry in the intrinsic state. It is interesting to investigate how this fascinating new state can be observed in experiments. The state with the torus configuration at J = 60 would have an extremely large magnetic moment ($\mu = 30\mu_N$). This would lead to a procession motion under an external magnetic field.

A question then arises how such a "femtoscale magnet" rotates spontaneously. When the spherical symmetry is broken, the collective rotation emerges spontaneously, in principle, to restore the broken symmetry. However, it is unclear whether such a state built with significant amount of circulating current can rotate about the perpendicular direction to the symmetry axis or not. If not, such a state would be an anomalous one, which has not yet been recognized in the experiments. Even if the state can rotate, the rotational band built on such a state would show interesting behaviors for their M1/E2 transition strengths and moment of inertia.

4. Time-dependent formation of nuclear pasta

The "pasta" phases of nuclear matter have been investigated intensively in various models, including Skyrme-force Hartree-Fock [10]. We have performed investigations in a time-dependent scenario to investigate the transition from some unordered initial state into the pasta phases depending on the density and temperature assumed initially [11].

For this purpose we set up a random initial state in a Cartesian periodic box. This state contained a number of α-particles at randomly selected positions (but rejecting positions with the particles too close) plus a background gas of neutrons in plane-wave states to produce a proton fraction of 1/3. Both the α-particles and the neutrons were given initial velocities from a thermal distribution. The typical grid consisted of 16^3 grid points with a spacing of 1 fm.

The calculated time dependence then showed a relatively rapid formation of one of the familiar pasta structures, which of course still contain time-dependence in the sense of vibrations remaining in the structures. This usually happens within less than 1000 fm/c. Since only a relatively small number of calculations could be performed, large fluctuations are present which, e. g., sometimes lead to different pasta structures for similar initial conditions.

While the average density is simply given by the number of particles in the computational grid, the temperature is given only indirectly. Since TDHF preserves the total energy, not the temperature, the latter has to be calculated for the final pasta configuration, which is not identical to the artificial temperature used to assign the initial velocities. In practice we estimated it by calculating the excitation energy relatively to the HF ground state and using the Fermi-gas formula. The resulting phase structure is shown in Fig. 8, while a graphical impression of the pasta structures attained is given in Fig. 9.

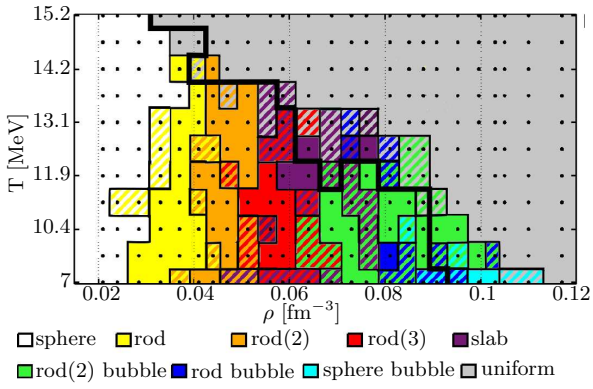

Figure 8. Phase diagram of the pasta structures reached in dependence on density and temperature. Taken from [11].

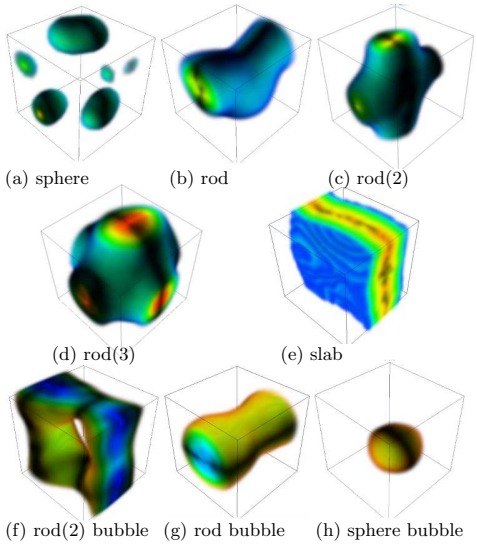

Figure 9. Overview of the pasta structures reached in the simulations. Blue color indicates the lowest and red the highest densities.

Since the geometric structure was quite complicated in many cases, we used the method of Minkowski scalars [12] to distinguish the various cases. This was already applied to similar situations in [13]. For this purpose the density threshold is selected to separate the system into "empty" and "filled regions" with clearly defined surfaces dividing them. Using these surfaces the geometric invariants can be calculated; we found the integral mean curvature and Euler characteristic most useful. The results are quite stable for a broad range of threshold densities. The main results are

summarized in the Table 1, which shows that indeed the classification can be done practically completely using just these two quantities.

Table 1. Classification of pasta configurations using the integral mean curvature and Euler characteristic. The letter "b" denotes the "bubble" configuration with high and low density regions exchanged.

Shape	Sphere	Rod	Rod(2)	Rod(3)	Slab	Rod(2) b	Rod b	Sphere b
W2	>0	>0	>0	- to +	≈0	<0	<0	<0
W3	>0	=0	<0	<0	=0	<0	=0	>0

Acknowledgments
This work was undertaken as part by the Yukawa International Project for Quark-Hadron Sciences (YIPQS), and was partly supported by the GCOE program "The Next Generation of Physics, Spun from Universality and Emergence" from MEXT of Japan. J.A.M. was supported by the Frankfurt Center for Scientific Computing and by the BMBF under contracts 06FY9086 and 06ER9063. One of the authors (JAM) would like to thank the Japan Society for the Promotion of Science (JSPS) for an invitation fellowship for research in Japan.

References

[1] Maruhn J, Kimura M, Schramm S, Reinhard P G, Horiuchi H and Tohsaki A 2006 α-cluster structure and exotic states in a self-consistent model for light nuclei *Phys. Rev.* C **74** 044311
[2] Ichikawa T, Maruhn J, Itagaki N and Ohkubo S 2011 Linear Chain Structure of Four-α Clusters in ^{16}O *Phys. Rev. Lett.* **107** 112501
[3] D'Agostino M 2011 Rod-Shaped Nucleus *Phys. Rev. Focus* **28** 10
[4] Wong C Y 1972 Toroidal nuclei *Physics Letters* B **41** 446–50
[5] Wong C-Y 1984 Rotating toroidal nuclei in heavy-ion reactions *Phys. Rev.* C **30** 1949–52
[6] Royer G, Haddad F and Jouault B 1996 Rotating bubble and toroidal nuclei and fragmentation *Nuclear Physics* A **605** 403–16
[7] Bohr A and Mottelson B R 1981 The structure of angular momentum in rapidly rotating nuclei *Nuclear Physics* A **354** 303–16
[8] Ichikawa T, Maruhn J A, Itagaki N, Matsuyanagi K, Reinhard P G and Ohkubo S 2012 Existence of exotic torus configuration in high-spin excited states of ^{40}Ca *Preprint* arXiv:1207.6250 [nucl-th]
[9] Wong C Y 1973 Toroidal and spherical bubble nuclei *Annals of Physics* **77** 279–353
[10] Newton W G and Stone J R 2009 Modeling nuclear "pasta" and the transition to uniform nuclear matter with the 3D Skyrme-Hartree-Fock method at finite temperature: Core-collapse supernovae *Phys. Rev.* C **79** 055801
[11] Schuetrumpf B, Klatt M A, Iida K, Maruhn J, Mecke K and Reinhard P-G 2012 Time-Dependent Hartree-Fock Approach to Nuclear Pasta at Finite Temperature *Preprint* arXiv:1210.8334 [nucl-th]
[12] Mecke K and Stoyan D 2000 *Statistical Physics and Spatial Statistics - The Art of Analyzing and Modeling Spatial Structures and Pattern Formation* vol 554 (Springer)
[13] Watanabe G, Sato K, Yasuoka K and Ebisuzaki T 2004 Phases of hot nuclear matter at subnuclear densities *Phys. Rev.* C **69** 055805